Mem. S.A.It. Vol. 79, 1267

Memorie della

Optically selected type-2 AGN: preliminary results from the COSMOS survey

A. Bongiorno[1], M. Mignoli[2], G. Zamorani[2], F. Lamareille[3], T. Contini[3], and the zCOSMOS team

[1] Max Planck Institut fuer Extraterrestrische Physik (MPE), Giessenbachstrasse 1, D-85748 - Garching bei Muenchen, Germany, e-mail: angelab@mpe.mpg.de
[2] INAF - Osservatorio Astronomico di Bologna, via Ranzani 1, 40127 - Bologna, Italy
[3] Laboratoire d'Astrophysique de Toulouse-Tarbes, Observatoire Midi-Pyrènèes, 14 avenue E. Belin, F31400 - Toulouse, France

Abstract. We present the first results on the type-2 AGN sample isolated from the zCOSMOS bright first observations of 10000 spectra. It is a purely magnitude selected sample with I<22.5. The sample consists of about 300 AGN, selected using the diagnostic diagrams in the redshift range $0.13 < z < 0.95$. We present a comparison of the optical and X-ray properties of these sources and a first preliminary determination of the luminosity function derived for this sample.

1. Introduction

According to the standard unified model (e.g. Antonucci, 1993), Active Galactic Nuclei (AGN) can be broadly classified into two categories depending on whether the central black hole and its associated continuum and broad emission-line region are viewed directly (type–1 AGN) or are obscured by a dusty circumnuclear medium (type–2 AGN). Type–1 AGN shows peculiar broad emission lines and are thus simply recognizable from their spectra. On the contrary, type–2 AGN have permitted and forbidden lines with similar widths (narrow lines) and have indeed spectra similar to normal star-forming galaxies (SFG).

Although the spectra of normal SFG and type–2 AGN are similar, the difference between them is in the ionizing source responsible for the emission lines: nonthermal continuum from an accretion disc around a black hole for what concern AGN or photoionization by hot and massive stars for normal SFG. The only way to isolate type–2 AGN is thus determine the ionizing source. Baldwin et al. (1981) demonstrated that this is possible by considering the intensity ratios of two pairs of relatively strong emission lines. In particular he proposed some diagnostic diagrams (hereafter BPT diagrams) then refined by Veilleux & Osterbrock (1987) based on [O III]λ5007Å, [O I]λ6300Å, [N II]λ6583Å, [S II]$\lambda\lambda$6717,6731ÅÅ, H$\alpha\lambda$6563Å and H$\beta\lambda$4861Å (where Hα and Hβ refer only to the narrow component of the line).

At high redshift, however, the involved lines (as Hα) are redshifted out of the observed optical range and the BPT diagrams cannot be used anymore.

Send offprint requests to: Angela Bongiorno

For this reason, Rola et al. (1997) and Lamareille et al. (2004) proposed new diagrams based on the strong lines [O II]λ3727Å, Hβ and [O III] which provide moderately effective discrimination between SFG and AGN.

In this paper we use these selection criteria to optically select and study a sample of type–2 AGN from the zCOSMOS survey. The selected sample consists of 258 objects at redshift 0.13 $< z <$ 0.95.

2. The zCOSMOS project

The zCOSMOS project is a large redshift survey that is being undertaken in the COSMOS field using 600 hours of observation with the VIMOS spectrograph on the 8-m VLT.

It consists of two parts: (a) zCOSMOS-bright, a magnitude-limited I-band $I_{AB} < 22.5$ sample of about 20000 galaxies with $0.1 < z < 1.2$ covering the whole 1.7 deg^2 COSMOS ACS field and designed to mimic the parameters of the 2dfGRS; and (b) zCOSMOS-deep, a survey of approximately 10000 galaxies selected through color-selection criteria to have $1.4 < z < 3.0$, within the central 1 deg^2.

For an exhaustive discussion of the zCOSMOS survey design, see (Lilly et al., 2007).

3. The type–2 AGN sample

The sample has been selected from the present zCOSMOS bright sample of 10000 objects after excluding duplicated objects, stars and broad line AGN. The starting sample was indeed of about 7085 sources. Then we extracted all the emission line galaxies in the explored redshift range ($0.13 \lesssim z \lesssim 0.95$) for which all the lines involved in the diagnostic diagrams, are measured with a signal-to-noise $S/N > 1$. The extracted sample consists of 3651 sources, 51% of the sample. Emission line equivalent width are measured using the automated software Platefit (Lamareille et al., 2008 in prep.) which does a simultaneous fit with a gaussian function of all the emission lines, after removing the stellar component. For these galaxies, we finally used the diagnostic diagrams to classify them in two main classes (star-forming galaxies and type–2 AGN) and we isolated and studied the type–2 AGN sample.

In the redshift range $0.13 < z < 0.45$, we used two BPT diagrams based on two-dimensional line-intensity ratios constructed from [O III]; [N II]; [S II]; Hα and Hβ. We will refer hereafter to these diagrams as *red1* and *red2* diagrams. We consider galaxies being SF or AGN combining together the two informations extracted from the *red1* and *red2* diagrams.

The exact demarcation between SFG and AGN in the BPT diagrams is subject to considerable uncertainty. In this redshift bin we assumed the theoretical upper limits on the location of SF models in the BPT diagrams found by Kewley et al. (2001), using a combination of photoionization and stellar population synthesis models.

In the redshift range $0.5 < z < 0.95$, we used the diagnostic diagram derived by Lamareille et al. (2004), [O III]/Hβ vs [O II]/Hα. The separation in this diagnostic diagram (hereafter *blue*) has been derived empirically on the basis of the data from the 2dFGRS. This diagram allows us to distinguish between AGN and SFG and moreover, since an intermediate region close to the demarcation is defined, we can also define two more regions of intermediate objects. In these diagrams we thus have also objects classified as candidate type–2 AGN or candidate SFG.

The total extracted type–2 AGN sample consists of 295 objects (90 Seyfert–2, 60 Seyfert–2 candidates and 145 LINER). SFG, lying below the curves, are the most numerous, making ~3356 (92%) of the sample while type–2 AGN constitute only 8% (295/3651) of the sample. Figure 1 shows the position of the sources in the three diagnostic diagrams used to classify them.

4. Comparison between optical and X-ray properties

Of our total analyzed sample, only 52/3651 objs (1.4%) have a X-ray counterpart (XMM catalog). In all our plots they are shown as crosses with different colors depending on the X-ray luminosity (black $Lx < 10^{42}$; grey

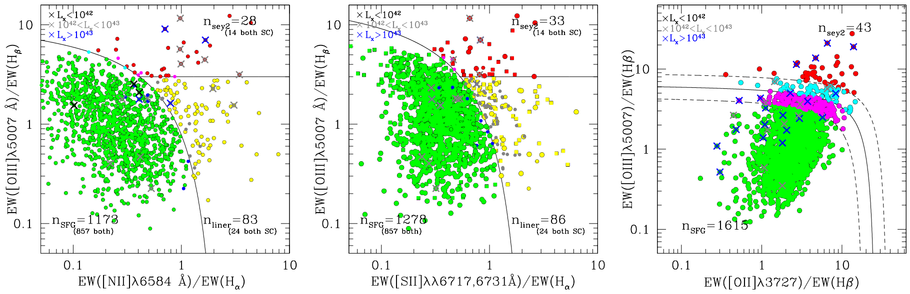

Fig. 1. (a) *red1*, (b) *red2* and (c) *blue* diagrams. Red circles correspond to objects classified as Sey–2, yellow to LINER, while green to SFG. Cyan circles and magenta circles are instead respectively candidate type–2 AGN and candidate SFG since they lie in the intermediate regions. Crosses mark X-ray detected objects and the different colors correspond to different X-ray luminosities.

$10^{42} < Lx < 10^{43}$; blue $Lx > 10^{43}$). 18 of them are optically classified as AGN while 34 of them are classified as SFG.

It is interesting to note that while the X-ray sources are distributed about randomly in the two red diagnostic diagrams, their position in the blue one is restricted to a defined region. Moreover, most of them and almost all the brightest sources ($Lx>10^{43}$), are in the SFG region ($Lx>10^{42}$ is the classical limit used to define a source as an AGN in the X-ray band).

A possible explanation for this distribution can be found in the composite models proposed by Stasińska et al. (2006). They proposed a model to quantitatively explain the distribution of observational points in the diagrams. This model suggests that objects that lie along the right wing of the diagrams, differ mainly in the balance between massive stars and AGN ionizing powers. They demonstrated that composite SF-AGN objects lie in the SF region of the diagrams until the AGN contribution is relatively high (e.g. in the red diagram, the Kewley separation line is passed when the AGN contribution is $\gtrsim$ 20%). In this framework, we could explain the position of X-ray sources in the diagrams, in particular the blue one (see fig. 4 of Stasińska et al., 2006), by assuming that they are composite objects.

To confirm this hypothesis, we computed the composite spectra of the SFG with and without X-ray counterpart. This is shown in figure 2. As you can see in this figure, the composite of SFG with X-ray emission (red spectrum) shows [Ne v] emission line which is a clear evidence of the presence of the AGN. This line is not present in the composite of SFG without X-ray emission. Moreover, the SFG with X-ray emission composite shows a redder continuum with respect to the other composite spectrum that can be explained as galactic extinction. Combining together these informations, the comparison of the two composites tell us that the X-ray sources that fall in the SFG region are probably AGN that are extincted on galactic scale.

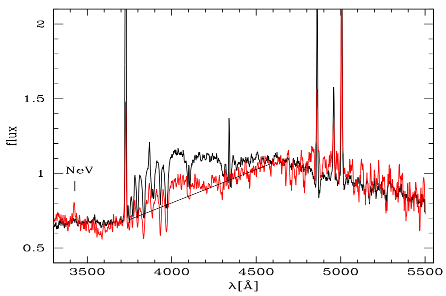

Fig. 2. Composite spectra of the star forming galaxies with (red line) and without (black line) X-ray counterpart.

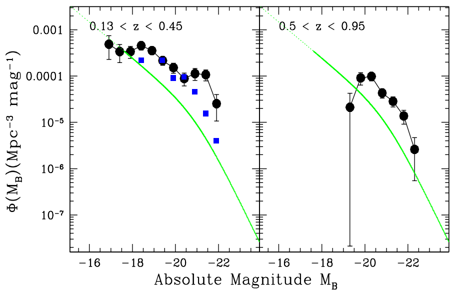

Fig. 3. Binned B-band LFs in two redshift bins derived from the zCOSMOS type–2 AGN sample (black circles). As comparison we show the binned LF at $z = 0$ from Ulvestad & Ho (2001) (blue squares) and the model derived by Hao et al. (2005) from a sample at $z < 0.13$ (green line)

5. Luminosity function

In order to study the evolution of type–2 AGN we derived the luminosity function (LF) from our sample. We computed a preliminary LF considering the B-band total magnitude. Since in the optical band, type–2 AGN are dominated by the host galaxy light, to sample and study only the light coming from the AGN, we should consider the [O III] line LF under the assumption that the [O III] line is purely of AGN origin. We will present it in a forthcoming paper (Bongiorno et al., 2008 in prep.)

We derived the binned representation of the LF using the usual $1/V_{max}$ estimator (Schmidt, 1968). Each volume V_{max} is also corrected for the incompleteness function which, for our sample, is made up of three terms linked, respectively, to (a) the selection algorithm used to design the masks, (b) the quality of the spectra and (c) the method adopted to select the sample.

The resulting LFs in different redshift ranges are plotted in Figure 3, where are plotted, as comparison, also the binned luminosity function derived from a sample of type–2 AGN at $z = 0$ selected from the Palomar spectroscopic survey (25 objs Ulvestad & Ho, 2001) and the model derived from the SDSS sample at $z < 0.13$ (Hao et al., 2005).

From the comparison with the SDSS model at low redshift, our LF data points suggest that the number of faint sources decrease going from z~0 to z~0.3 while the number of bright sources increase. The extrapolation of the Hao's model fit indeed overestimates the faint part of our luminosity function and underestimates the bright part.

At higher redshift (z~0.7), the excess of bright sources disappears and the faint part of the LF is not so well constrained to see a possible trend.

As already mentioned, a [O III] line LF will give us more constrains on the AGN evolution. However, from this estimation of the LF, it is possible a direct comparison with the LF of the total zCOSMOS galaxy sample (Zucca et al., private communication). From this comparison, we found that the fraction of galaxies that shows AGN activity is ~5% at these redshifts.

References

Antonucci, R. 1993, ARA&A, 31, 473
Baldwin, J. A., Phillips, M. M., & Terlevich, R. 1981, PASP, 93, 5
Hao, L., Strauss, M. A., Fan, X., et al. 2005, AJ, 129, 1795
Kewley, L. J., Dopita, M. A., Sutherland, R. S., Heisler, C. A., & Trevena, J. 2001, ApJ, 556, 121
Lamareille, F., Mouhcine, M., Contini, T., Lewis, I., & Maddox, S. 2004, MNRAS, 350, 396
Lilly, S. J., Le Fèvre, O., Renzini, A., et al. 2007, ApJS, 172, 70
Rola, C. S., Terlevich, E., & Terlevich, R. J. 1997, MNRAS, 289, 419
Schmidt, M. 1968, ApJ, 151, 393
Stasińska, G., Cid Fernandes, R., Mateus, A., Sodré, L., & Asari, N. V. 2006, MNRAS, 371, 972
Ulvestad, J. S. & Ho, L. C. 2001, ApJ, 558, 561
Veilleux, S. & Osterbrock, D. E. 1987, ApJS, 63, 295